MONABIPHOT

Master Thesis by

Rachel L. Warnock

rachellwarnock@gmail.com

Bioluminescence-Triggered Bacterial Adhesion as a Sensor for Inorganic Mercury

Host Institution

Max Planck Institute for Polymer Research

Wegner Lab Group

Ackermannweg 10, 55128 Mainz, Germany

Supervisor

Dr. Seraphine Wegner

wegners@mpip-mainz.mpg.de

10.07.2019

Abstract

This project utilizes the bioluminescence output of a whole cell mercury sensor to trigger bacteria-bacteria adhesions and aggregation as the transducing element of the sensor. In the design, *E. coli* were engineered to generate bioluminescence in response to Hg^{2+} ions with a merR-lux transcriptional fusion and to express one of the photoswitchable proteins nMagHigh or pMagHigh on their surfaces. This blue luminescence was used to activate the blue light dependent heterodimerization the proteins nMagHigh and pMagHigh and results in the adhesion of the bacteria to each other and bacteria to settle out of solution in large (>15 μm^2) clusters (see Figure 0.1). This aggregation increased with increasing Hg^{2+}/bioluminescence and was even higher than bacteria activated directly by blue light. Moreover, the endogenous bioluminescence also induced larger clusters than under blue light. The clustering size and degree of aggregation was influenced by the concentration of $HgCl_2$. Finally, the mercury dependent bioluminescence output also increased biofilm formation. Overall, combining the bioluminescence output of merR-lux and the photoswitchable proteins in concert, the bacteria can concentrate onto a substrate, offering potential for improved heavy metal detection in whole-cell biosensors.

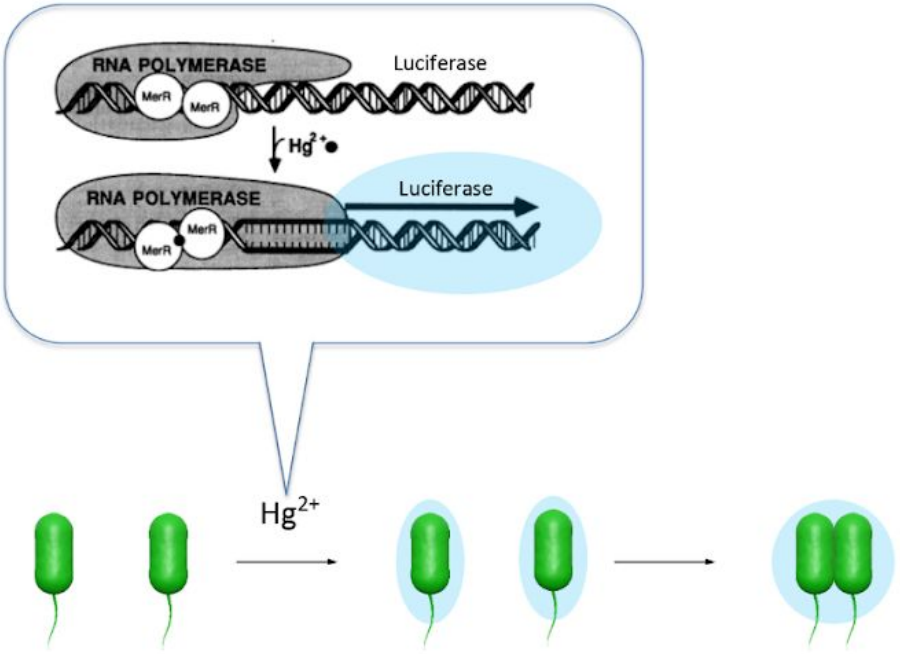

Figure 0.1. Schematic of the project showing bacterial clustering in response to Hg^{2+}

Acknowledgements

I would first like to thank my Group Leader and advisor, Dr. Seraphine Wegner for accepting me into her group and guiding me through this project. I also thank Prof. Dr. Landfester for her leadership of the working group.

I also could not have completed this project without the guidance of my PhD student advisor, Fei Chen. Thank you for being an extensive source of knowledge and advice, but also for being kind and always willing to discuss about careers or culture.

I would like to thank Marc, Dongdong, Brice, Ilke, Samaneh, Taniya, and Sukant for being great lab mates. They were a social community during work and breaks and a source of knowledge and experience. Additionally the other members of the Landfester group for networking opportunities and social events that provided entertainment and cultural exchange in Mainz.

Thank you to Prof. Dr. Ledoux for all her work coordinating the MONABIPHOT program throughout various complicated situations. She has always been kind and accommodating even in times of stress. Thank you for doing what you are doing and making this experience possible for me.

I thank the professors in Cachan, Madrid, and Wroclaw for providing guidance both in understanding scientific concepts, and in professional and personal goals. I am grateful for all the timely letters that were written on my behalf in order to secure visas. I especially thank Prof. Dr. Katarzyna Matczyszyn for opening up her home and allowing me to be a part of her family on Christmas.

Thank you to Juan Jose, Momoko and Julia for being teammates, study/lab partners, roommates, travel companions, and confidants. Thank you to Dominika, Sebastian, Manuela, and Pawel for being so hospitable in Poland: from housing advice to helping me navigate interactions with the Foreigner's Office.

I thank my family and friends who supported me in my decision to move abroad and have continued supporting me through all the ups and downs.

I am grateful to the Erasmus Mundus program for providing the funding for my scholarship. These two years abroad have catalyzed an incredible amount of personal and professional growth for me I could not have gotten with any other path.

Table of Contents

Chapter 1 – Introduction

Biosensors

As the world utilizes more global transportation and industrialization, toxic chemicals and pollutants have increased contact with humans and the environment. Heavy metals pollute the environment from both anthropogenic sources and natural processes, presenting a danger to organisms. Mercury can be found in environmental samples in three forms: elemental Hg^0, inorganic Hg compounds, and as an organomercury compound, like monomethylmercury (MeHg). Each form, along with each dose or delivery method presents a unique risk for mercury exposure.[1] Inorganic, divalent Hg^{2+} is often used in products such as antiseptics and teething creams. Direct exposure to as little as 1g can be fatal to an adult as inorganic mercury accumulates in the kidneys, liver, and nervous system.[2] Because heavy metals, such as mercury, can cause such harm to human health and greater ecosystems, quick and accurate detection systems are valuable developments.

Generally, methods of monitoring and detecting hazardous substances can be classified in two categories. The first is instrument-based analytical methods. These precise monitoring systems include gas chromatography (GC), high-performance liquid chromatography (HPLC), inductively-coupled plasma/mass spectrometry (ICP-MS), atomic absorption spectrometry (AAS), and more. These instruments are very accurate and can detect small concentrations of toxicants, but they are expensive, complex, and require lengthy sample preparations.

The second approach to monitoring hazardous materials is biosensors.[3] Biosensors utilize a biological element for recognition, such as an enzyme, protein, or a whole cell, in combination with a transduction element, such as a thermal or optical output, to provide quantitative information about the bioavailable metal.[4] Cell-free systems often involve an analyte binding to a biological element, like a peptide or enzyme, deposited onto a substrate. Thus, these systems require purification and expression steps that increase the effort required when compared to biosensors utilizing whole cells. Whole cell biosensors are easy and cheap to cultivate and require no complex techniques to be analyzed.[3]

In addition to bacterial cells being excellent potential vehicles for sensing from an efficiency perspective, these organisms are advantageous for other reasons. Bacteria are capable of mobilizing many forms of mercury, allowing this toxic agent to bioaccumulate in other organisms throughout the food web.[1] Further, only a portion of "bioavailable" mercury in environmental media is actually able to be solubilized and taken up by the surrounding organisms. This bioavailable portion that can accumulate in organisms likely to be eaten or contaminate humans is necessary for evaluating the risk of a toxin. When whole bacterial cells are used as sensors that detect target ions with gene fusions expressed in the cells' cytoplasm, then these sensors evaluate the amount of the ion that is available for transformation.[5] Thus, utilizing whole bacterial cells as sensors and reporters of mercury in samples is an effective evaluation of bioavailable mercury.[6] These sensors need to be robust and sensitive in order to detect the small, yet harmful, levels of mercury present.[4] Additionally, ideal biosensors (not only bacterial) should be designed to exhibit high sensitivity and specificity in a reproducible manner. These parameters should additionally be verified by different experimental methods. Total bioluminescence or fluorescence emitted from whole cell biosensors can estimate the response to analytes. Measuring the total light emitted could be influenced by cell heterogeneity within the biosensor batch, or signal interference. To minimize these problems, genetic elements to influence the movement of cells based on their response to an analyte could be introduced.[3]

MerR as a Sensing Element

MerR is a family of transcriptional regulators controlling the gene expression related to metal ion detoxification, efflux, and sequestration. For example, the merA gene encodes for a mercuric reductase, which reduces Hg^{2+} into the less-toxic metallic form Hg^{0}.[7] The merR protein functions as a regulator of the mercury resistance operon Tn21, which encodes for many other merR family proteins. MerR sits on the mercury resistance operon as a repressor of transcription, thus transcription of these genes only occurs through protein-dependent DNA distortion.[8] MerR is a homodimer made up of a metal binding domain (MBD), a DNA binding region, and a coiled-coil domain. The MBD confers high specificity and sensitivity due to its unique configuration of three conserved cysteine residues of two monomers in a trigonal planar conformation.[9] When a target metal ion (Hg^{2+}) binds in the MBD, this causes a

distortion in the bound duplex DNA of the operon, which causes the DNA to unwind. In natural systems, this initiates transcription of genes for proteins that will pump Hg^{2+} into the cell and reduce it to a less harmful form in order to mitigate the toxic effect (see Figure 1.1).[7] In this case, the resistance genes (Tn21 operon) have been replaced with the luciferase enzyme reporter (lux operon). Thus, when the merR complex binds to Hg^{2+} ions, repression of the lux genes is removed, and luciferase will be generated by the cell. When luciferase catalyzes the oxidation of its reactants, this generates intense luminescence around 485nm.[7] This light is the reporter function in many sensor configurations. Thus, a mercury resistance operon can utilize luciferase (merR-lux) to detect mercury ions in solution.

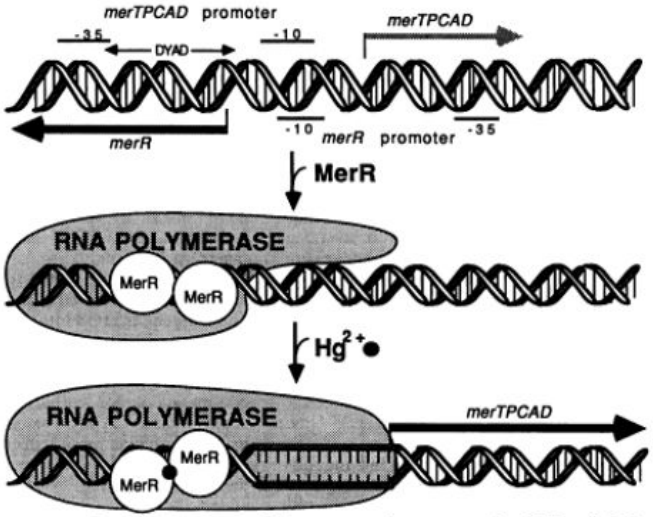

Figure 1.1 Scheme of merR activating/repressing action with Hg^{2+}. Relative expression of the promoter downstream from the merR binding dyad is shown with the arrow thickness.[7]

Luciferase / Bioluminescence

Luciferases are a class of enzymes which emit bioluminescence upon acting on their substrates. There are several different natural sources of luciferase. Bacterial luciferase has been observed in several microorganisms, including *Vibrio harveyi*, *Vibrio fischeri*, and *Vibrio haweyi*. The luciferase enzyme catalyzes the oxidation of the reduced form of flavin mononucleotide ($FMNH_2$) and myristyl aldehyde (RCHO) into myristic acid (RCOOH) and flavin mononucleotide (FMN) (see Figure 1.2).[10] An additional result of this reaction is a liberation of light with a wavelength of 485 nm.

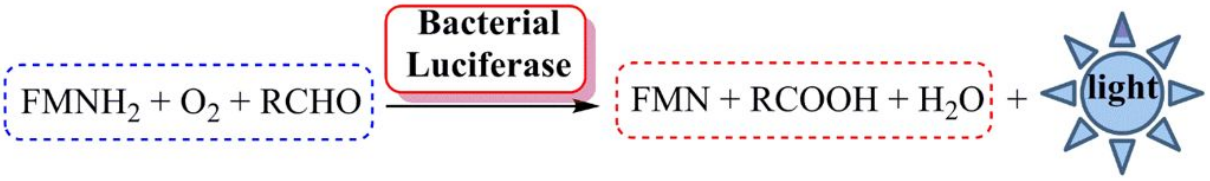

Figure 1.2: Depiction of oxidation reaction emitting luminescence[10]

The second type of luciferase is known as firefly luciferase, and catalyzes a two-step oxidation reaction. Using ATP as a cofactor, luciferin is converted into luciferyl-adenylate, and then oxidized into oxyluciferin. When luciferin is broken down, a byproduct of this process is an emitted photon, which can be detected in the wavelength range of 550-570 nm.[11] Firefly luciferase requires the addition of an external substrate; However, bacterial luciferase lux operons have been designed to include luxCDE, which allows the bacteria to produce a decanal substrate endogenously, required for the enzyme's function.[12]

This bioluminescent light emission has been utilized in biotechnology as a reporter for promoter activity without the need for incident light, as is the case for fluorescent reporters. However, there are benefits to luminescence over fluorescence. For example, Huang, et al. showed that in terms of metal sensitivity, luminescence is a more accurate reporter signal than fluorescence. In this case, the Limit of Detection (LOD) in a whole-cell biosensor of a gfp-based construct was four times higher than that of a lux-based construct used in the same biosensor cells.[12] Bioluminescence from the lux operon is an excellent option for the transduction element component of a biosensor.

Controlling Cell Adhesion with Light

The second goal of this work, bacterial adhesion and aggregation, can be achieved by the action of photoswitchable proteins. Photoswitchable proteins are excellent tools for optogenetics because their interactions are very specific and can respond to visible light, even at low intensities. The proteins can be genetically encoded, allowing stable expression in the cells. Using light as a switch brings excellent spatial and temporal control to cellular interactions. For example, in the following system, cells will aggregate when the light

stimulus has been applied.[13] However, the goal of the project is to induce this photoswitching action in the presence of mercury/ merR-induced bioluminescence, not external light.

The photoswitch pairs chosen for this project are known as Magnets, derived from the Vivid (VVD) fungal photoreceptor. The VVD photoreceptor is one of the smallest photoreceptors as optogenetic tools, and uses flavin adenine dinucleotide (FAD) as its cofactor, which is common in eukaryotes (see Figure 1.3). When exposed to blue light, the Cys108 forms a photo-adduct with the isoalloxazine ring of FAD, which causes dimerization. This dimerization can be used to control protein-protein interactions. Kawano, *et al.* developed two forms of VVD variants, called Magnets. This pair of Magnets known as nMag and pMag, respectively responds to blue light (480 nm) by heterodimerizing, and will dissociate in the dark. The pair was designed to recognize each other based on electrostatic interactions, thus homodimerization is reduced. In addition to engineering the dimerization of this VVD pair, the switch-off kinetics of the pairs were tweaked, so the kinetics of the interactions could also be controlled. [14] The point mutants known as nMagHigh and pMagHigh have been utilized due a stronger partner interaction than the regular nMag/pMag pair.[13]

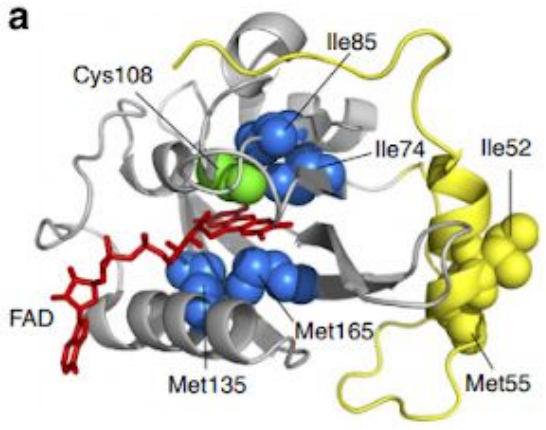

Figure 1.3. Scheme showing VVD's structure. Dimerization occurs when light triggers the Cys108 (green) and part of the Flavin adenine dinucleotide (FAD, red) to come together to form a photo-adduct.[14]

The pair of Magnet proteins can each be expressed and presented on the exterior of the cell membrane in order to cause adhesion of different cells. Fusing the magnet proteins with the enhanced circularly permuted transmembrane/outer membrane protein eCPX effectively achieves this. After bacteria is transformed with such a construct, the eCPX scaffold can

display peptides in high efficiency in a short time with an arabinose treatment.[15] After the Magnet proteins are displayed on the cell's exterior, the protein pairs can recognize each other through electrostatic interactions during the random collisions occurring in mobile bacteria.[14] *E. coli* is a model organism for studying cell aggregation and biofilm formation.[16] Aggregation can be observed as microscopic cell clumps emerging, then growing into macroscopic flocculation and settling out of static liquid culture.[17] Together, these components allow for an effective study of control over cell adhesion and aggregation in response to light.

Chapter 2 – Experimental

Material

The plasmid pB33eCPX, which contains the gene for the enhanced circularly permutated outer membrane protein eCPX, was a gift from Prof. Patrick Daugherty (Addgene plasmid # 23336).[15] *E. coli* DH5α carrying the pPROBE-merR-egfp and pPROBE-merR-lux plasmids, respectively, were gifts from Prof. Dr. Jan van der Meer. The nMagHigh gene in the pET-21b(+) plasmid between the NdeI and XhoI cutting sites was purchased from Genescript. In previous work, Fei Chen fused the nMagHigh and pMagHigh separately to the N-terminal of eCPX in the pB33eCPX plasmid to express the appropriate protein on the *E. coli* surface.[13] *E. coli* K12 MG1655 was purchased from DSMZ. The Hoechst 33342 nuclear counterstain was purchased from Thermo Fisher. All enzymes were purchased from New England Biolabs and all other chemicals were purchased from Sigma-Aldrich.

Bacterial Culture

E.coli K12 MG1655 were co-transformed with one of the eCPX-fused photoswitchable protein plasmids (nMagHigh-eCPX or pMagHigh-eCPX, chloramphenicol resistant, *L*-arabinose inducible) and the mercury detection protein expression plasmid (pPROBE-merR-lux, tetracycline resistant). 5 mL LB medium containing 20 µg/mL chloramphenicol, 10 µg/mL tetracycline, 0.04% m/v *L*-arabinose, and 1.25 mM $HgCl_2$ when applicable was inoculated with a single colony and incubated in the dark overnight at 37 °C at 130 rpm. After 15 hours, the bacteria were diluted in PBS (phosphate buffer saline) to an optical density of 0.15 for use in further studies.

Luminescence Assay

To assess the luminescence in response to different concentrations of $HgCl_2$, bacteria was cultured overnight as described. After 15 hours, a subculture was prepared with 200 µL

of the overnight culture, 10 mL LB, 20 µg/mL chloramphenicol, and 10 µg/mL tetracycline and incubated at 180 rpm and 37°C for about 2 h, when the OD_{600} is roughly 0.4-0.6. The culture tubes were then centrifuged at 25°C and 3500 rpm for 7 minutes. The supernatant was removed and replaced with 5 mL LB, then the pellet was dispersed using a P1000 pipette. Separately, a calibration series of $HgCl_2$ was prepared at the following molarities: 1.25, 2.5, 12.5, 49.9, 124.6, 498.5, and 1246.3 nM. 15 mL Falcon tubes were prepared with the following: 1.2 mL of this concentrated cell suspension, 400 µL LB, 2 mL PBS, 0.04% m/v *L*-arabinose, and 400 µL selected mercury solution. The tubes were incubated in the dark with slightly unscrewed caps at 100 rpm and 30°C for 3 h. 200 µL of each concentration were transferred into a 96-well plate. The luminescence intensity in the blue region was then measured by a Tecan M1000 Infinite® microplate plate reader. A calibration curve was constructed using Excel.

Specificity & Toxicity Assays

Bacteria were cultured as previously described overnight, then concentrated doubly by centrifuging the falcon tubes at 3500 rpm at 25°C for 7 minutes, removing the liquid, and re-dispersing the pellet of cells in 2.5 mL of PBS. Stock solutions (1 M) of the following metals were prepared: $NiCl_2$, $CoCl_2$, CuCl, $ZnCl_2$, $PbCl_2$, $FeCl_2$, and $HgCl_2$. 15 mL Falcon tubes were prepared with the following: 600 µL concentrated cells, 200 µL LB, 1 mL PBS buffer, and 200 µL of selected metal (final concentration of 1.25 mM). Tubes were incubated at 130 rpm and 37°C for 2 hours. At the end of incubation, 200 µL of each were transferred into a 96-well plate, as well as PBS blanks. Each well was analyzed for blue luminescence and absorbance at 600 nm using a Tecan M1000 Infinite® microplate plate reader. Data was corrected by subtracting the blank from each value.

Bacterial Aggregation Assay

After the *E. coli* cultures were diluted, Hoechst 33342 was added at a 1:1000 dilution of 10 mg/mL working concentration and thoroughly dispersed by pipetting. Bacteria displaying nMagHigh were mixed in a 1:1 ratio with *E. coli* displaying pMagHigh (OD_{600}=

0.15). Then, 300 µl of the mixed bacterial culture was added into 8-well slides (µ-Slide, 8-well glass bottom; ibidi), mixed by pipetting, and incubated for 2 h. Positive controls were not exposed to mercury, but instead were set under blue light illumination (270 µW/cm^2); all other samples were kept wrapped in foil to prevent light contamination.

Images were acquired on an inverted Confocal Laser Scanning Microscope (CLSM, Leica TCS SP8) equipped with a 405 nm laser for excitation of the Hoechst staining, a photomultiplier detecting emission from 460-550nm, and a 40x objective. For each sample, 25 images (Voxel size of 0.284 µm) were acquired with both bright field and fluorescent channels. These images were then analyzed using the image process tool FIJI (FIJI, https://fiji.sc/). Using FIJI, brightness and contrast were automatically adjusted to help identify cells. The image thresholds were adjusted using the automatic method and by conversion, binary images were generated. Using the particles analysis function, clustered bacteria and all bacteria (single and clustered) in each image were detected by measuring objects with an area > 15 µm^2 and > 2 µm^2, respectively. To quantify these results, aggregation ratio (the sum of the area occupied by clustered bacteria area > 15 µm^2 / sum of area occupied by all bacteria > 2 µm^2) was chosen. The average sizes of clusters were also utilized, obtained using the results from the particle analysis tool.

Biofilm Formation Assay

Overnight cultures of *E.coli* displaying nMagHigh and pMagHigh were diluted in LB to OD_{600} 0.01 with LB containing 20 µg/mL chloramphenicol, 10 µg/mL tetracycline, 0.04% m/v *L*-arabinose and 1.25 mM $HgCl_2$ when applicable. 200 µl of bacterial co-cultures were added in a 1:1 ratio to a 96-well plate (Greiner Bio-one, round bottom). After 48 h of incubation under blue light (135 µW/cm^2) or in the dark at 37°C, the wells were rinsed with H_2O and 200 µl of 1% crystal violet (CV) solution was added to each well. After 15 min incubation at room temperature, the wells were rinsed thrice with H_2O. The remaining crystal violet was solubilized by adding 200 µl of 30% acetic acid in water, and after 15 minutes, this solubilized CV was transferred to a new flat bottom 96-well microplate. Absorbance was quantified in a plate reader at 550 nm using 30% acetic acid in water as the blank.

In parallel, 300 µl of bacterial co-cultures were added in a 1:1 ratio to 8-well slides for imaging. The slides were also incubated under blue light (135 µW/cm^2) or in the dark at 37 °C

for 48 h. The slides were then rinsed in diH_2O once and imaged by CLSM Leica TCS SP8 with stacks scanning. Stack scanning images of biofilms were analyzed with 3D reconstruction by the Leica software.

Chapter 3 – Results and Discussion

Initial Investigations

Mercury-Dependent Bioluminescence in DH5α

Plasmids received both used GFP and lux, respectively, as the reporter signal in response to sensing mercury in solution. The plasmids were transformed into the *E. coli* strain DH5α for initial studies. This strain is appealing for preliminary studies because it has been engineered for stable DNA amplification and optimized transformation efficiency.[21] Upon successful transformation and culturing, the reporting signal output in response to $HgCl_2$ solutions was tested. Calibration curves were generated by carrying out luminescence assays with different concentrations of $HgCl_2$ for both bacteria transformed with pPR-merR-gfp (fluorescence) and pPR-merR-*lux* (luminescence), respectively. As seen in Figure 3.1, linear trendlines could be fit to both of these datasets. These curves indicate good sensitivity of the fluorescent and luminescent transduction elements in response to merR binding to Hg^{2+} ions. This investigation also demonstrated an increase in signal intensity with an increase in $HgCl_2$ concentration. Based on this, the highest level of mercury (1.25 mM) was chosen for future experiments with aggregation because of the high luminescence intensity generated.

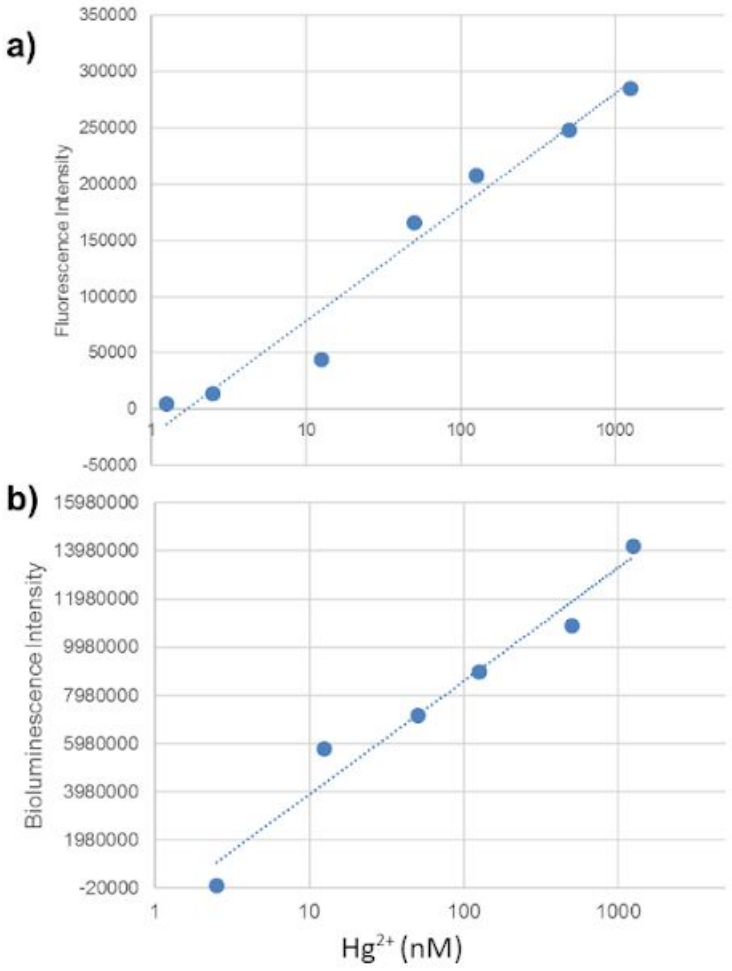

Figure 3.1. Graphs showing the calibration curves with different concentrations of mercury. a) Fluorescence from merR-gfp b) Luminescence from merR-lux

Mercury-Dependent Bioluminescence in MG1655 Co-Expressing Magnets

After confirming the functionality of the system in the accessible DH5α strain, the next step was to co-transform the merR plasmids and the Magnet protein plasmids into *E. coli* strain MG1655. This strain was preferable for these studies due to its movement capabilities, as motility is required not only to provide collisions for Magnet proteins to attach, but also because this is the first step in forming a biofilm.[19] It was necessary to investigate any effects of co-expression on the generation of bioluminescent signal in order for future experimentation to proceed. When the merR-lux or merR-gfp plasmids were co-expressed in MG1655 *E. coli* along with each respective magnet pair (nMagHigh or pMagHigh), the sensing ability was tested. By performing a calibration test using different concentrations of mercury, the signal output was measured to ensure that magnet co-expression caused no

impedance to the merR system in its ability to sensitively detect mercury. Both bioluminescence and fluorescence could be detected in response to very low levels of mercury (see Figure 3.2).

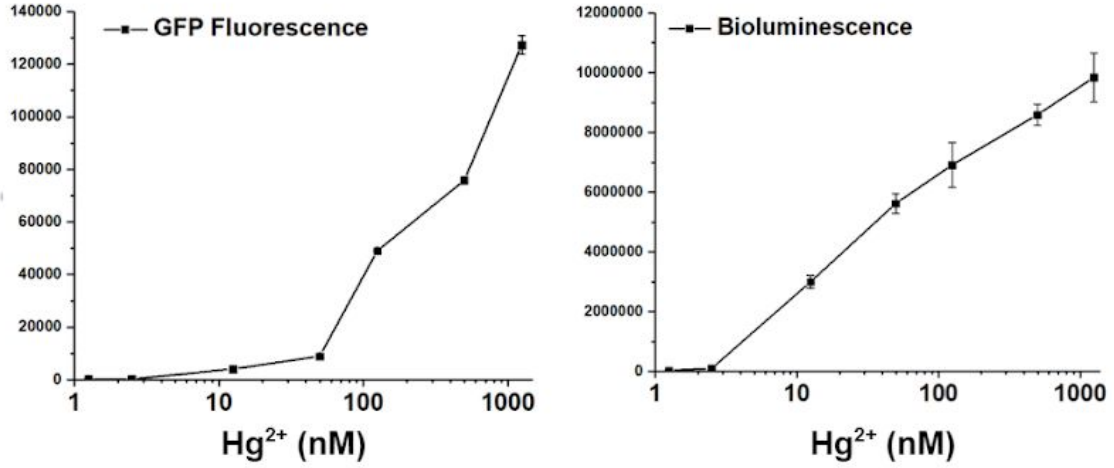

Figure 3.2. Graphs showing the calibration curves with different concentrations of mercury in the MG strain and Magnets co-expressed a) Fluorescence from merR-gfp b) Luminescence from merR-lux

Both experiments were performed on the same plate reader unit, so their noise level and instrumental limit of detection are standard. Luminescence detection yields a largely linear graph with a high slope, which indicates good ability to sense low concentrations of mercury. The standardly-used levels of Limit of Detection (LOD) and Limit of Quantification (LOQ) could be applied in this case (see Equation 3.1).[18]

$$LOD = 3 * \sigma_{\text{blank}}$$

$$LOQ = 10 * \sigma_{\text{blank}}$$

Equation 3.1. Standard equations for Limit of Detection and Limit of Quantification

The LOD and LOQ for the bioluminescence signal measurement were 0.9662 and 0.9663 nM of mercury, respectively. For the fluorescence signal, the LOD calculated was 134.6 and the LOQ was 448.6 nM Hg. Concentrations above these lower limits were chosen for further experimentation in order to increase luminescent signal generated.

Lack of Toxicity

To further investigate the co-expressing bacteria system, another experiment was devised. To ensure no harmful impact on growth was occurring due to the short term exposure to a heavy metal, the optical density at the end of a typical luminescent assay culturing time was measured with the same concentrations of different ionic species. The optical density at the end of culturing did not change significantly based on ionic identity. This indicates that any toxic effect caused by the heavy metal did not take place during assay time and does not impact the outcome of the study.

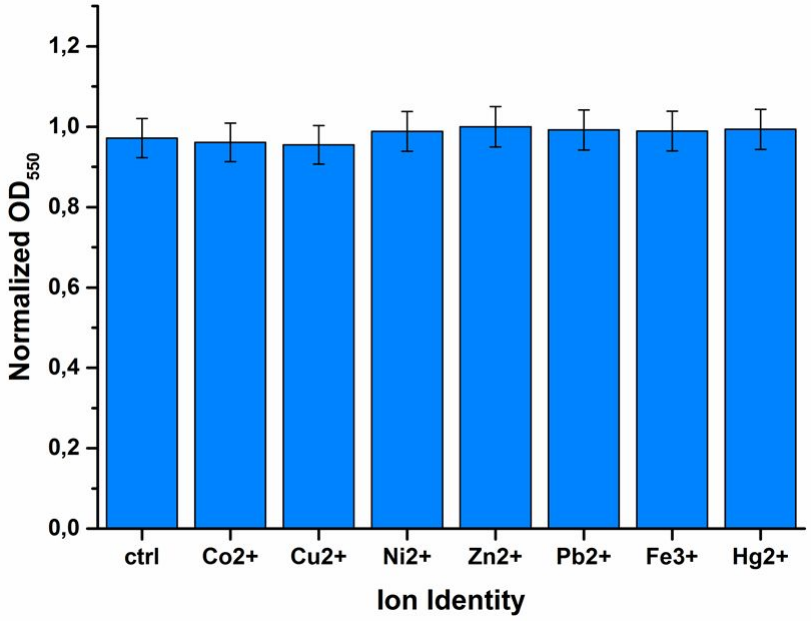

Figure 3.3. The normalized optical density (OD) of bacteria cultivated for hours with different metal ions

Specificity

The merR family of proteins is known to be especially specific due to the MBD's unique trigonal planar configuration of three conserved cysteine residues of two monomers.[9] However, it was necessary to incubate the two plasmid bacterial system with other metallic ions and measure bioluminescent output as a test. As seen in Figure 3.4, adding ions other than mercury (at the same concentration) induced only a negligible level of luminescence. This confirms the specificity of the merR binding site.

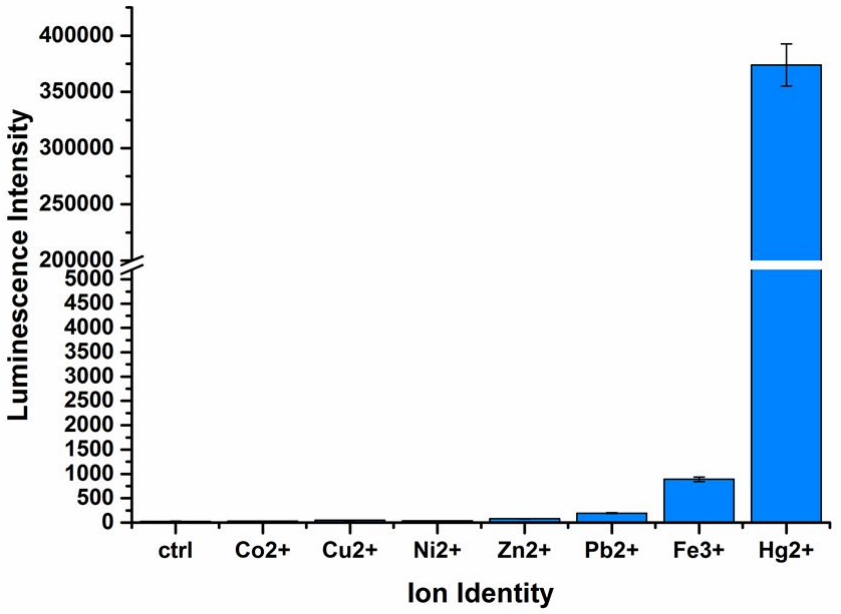

Figure 3.4. Bioluminescent intensity after incubation for 2 hours with different ionic species.

Aggregation Studies

In order to investigate the hypothesis, aggregation studies were carried out as previously described. Confocal microscopy yielded images that clearly show large clusters > 15 μm^2 that have settled to the bottom of the wells in the case of blue light and mercury (see Figure 3.5). The bacterial staining with Hoechst dye allowed these images to be quantified. The ratio of bacteria in the images that are a part of a large cluster to the total amount of bacteria present is known as the aggregation ratio. Highest aggregation ratios resulted from the Hg^{-}exposed samples, indicating a high level of clustering due to the mercury treatment. Bacteria under blue light aggregated more than the dark negative control sample, but less than the luminescent experimental sample. Not only did these samples cluster the most, the size of these clusters was also greater than the clusters formed in blue light. It is clear that bacteria-generated lux bioluminescence is a more effective inducer of Magnet adhesion than traditional blue light.

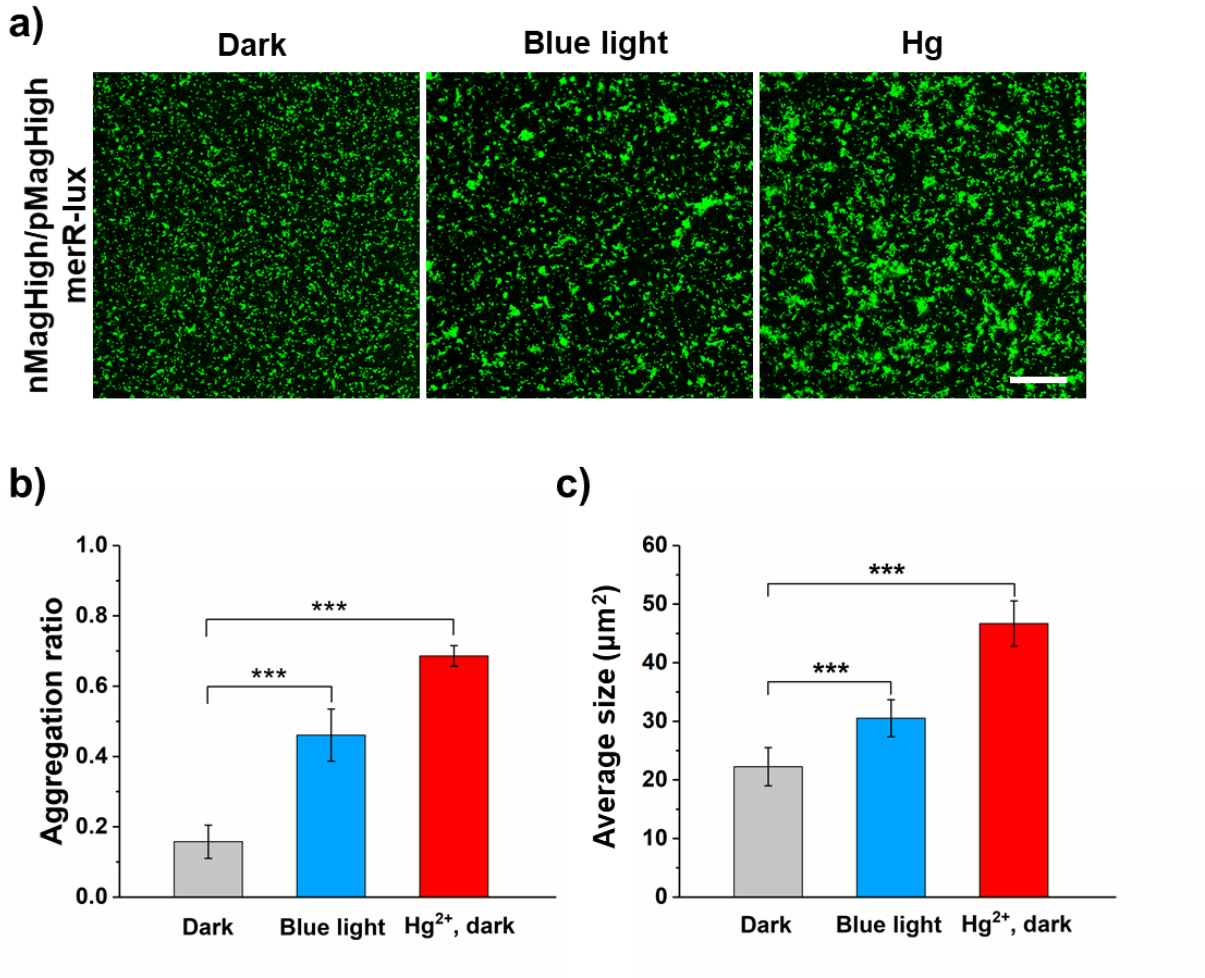

Figure 3.5. Aggregation of bacteria in response to light. a) confocal images with Hoechst dye showing clusters. Scale bar is 50 µm. b) Quantified aggregation ratios (*** = $p<0.001$) c) Average size of clusters > 15 μm^2

After confirming that mercury-generated lux bioluminescence could induce aggregation better than traditional LED light sources, this control was explored. Two concentrations lower than the 1.25 mM concentration used in the previous aggregation studies were chosen. By comparing aggregation between different concentrations of $HgCl_2$, the level of control over cell adhesion could be investigated. As seen in Figure 3.6, lower levels of mercury resulted in less aggregation and the clusters that did form in this case were smaller.

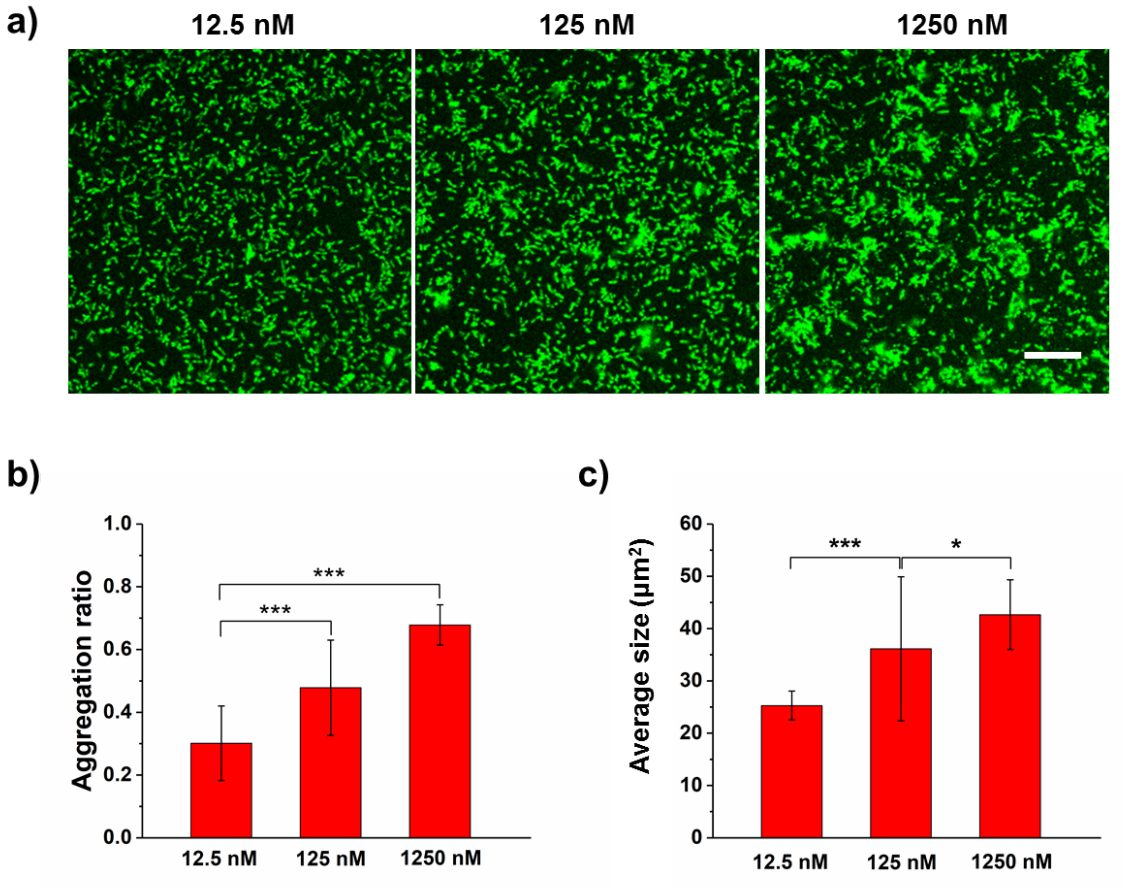

Figure 3.6. Response on clustering from different mercury concentrations. a) confocal images with Hoechst dye showing clusters. Scale bar is 100 µm. b) Quantified aggregation ratios (*** = $p<0.001$, * = $p<0.05$) c) Average size of clusters > 15 μm^2

Biofilm Formation

In order to further test the hypothesis that biogenic, Hg^{2+}-triggered bioluminescence can induce cell adhesion and aggregation, which leads to cell clusters settling out of solution, the next experiment devised was to test if these settled cells would eventually form a collective biofilm. In natural systems, different microorganisms typically exist attached and grown onto surfaces. However, biofilms are more than just a layer of bacteria. Biofilms form when microbes attach irreversibly to a surface, growing, producing extracellular polymers and matrices, and communicating and coordinating with the community through methods such as quorum sensing. Ultimately, organisms involved in a biofilm have altered phenotypes compared to free swimming organisms with respect to growth rate and genetic transcription.[20] This collective community of bacteria allows these microbes to be more resistant to

environmental stress, and confers them with an advantage for survival. Bacterial adhesion that progresses into the formation of a biofilm presents stronger proof of control over cell adhesion due to photoswitchable interactions.[13]

After exposing appropriate culture mixes to the three conditions as detailed previously, biofilms formed. Bright field imaging in three dimensions yielded images that clearly show the difference in treatment results and also thickness measurements could be taken (see Figure 3.7). The average dark negative control biofilm thickness was 14.142 µm, the positive blue light control was 18.45 µm, and the average experimental Hg sample thickness was 30.6 µm. Additionally, the optical density measured from the crystal violet staining used showed significant increase in biofilm formation between the negative control and Hg or blue light-exposed samples.

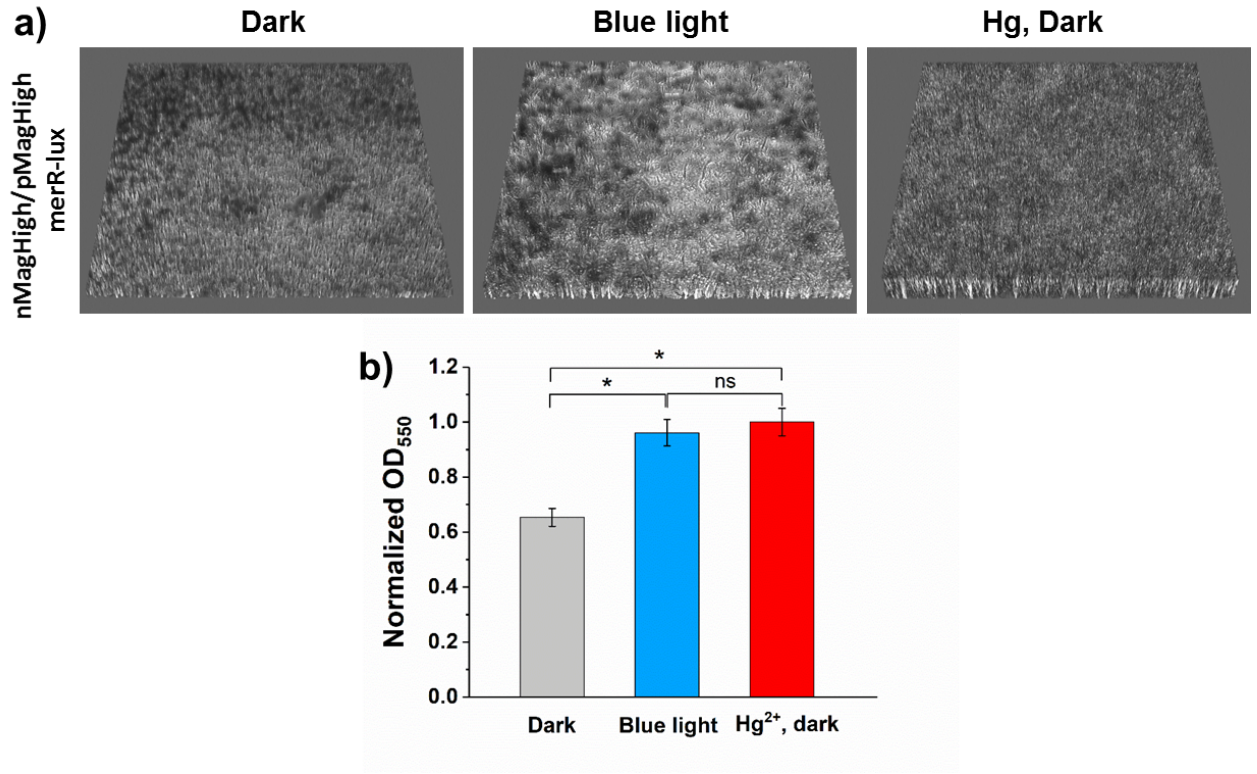

Figure 3.7. Biofilm formation images. a) 3D bright field images taken at 40x objective. b) The optical density of biofilms grown (* = $p<0.05$)

Chapter 4 – Concluding Remarks

This project utilizes a whole cell mercury sensor to impact bacterial adhesion and aggregation as the transducing element of the sensor. Thus, the need for a light input while detecting heavy metals like mercury in low concentration is eliminated. When Hg^{2+} ions are present in solution, they interact with the merR-lux component, activating the lux bioluminescence. This signal generated from the bacterial cells themselves acts as the catalyst for heterodimerization of Magnet protein elements. Thus, binding of the nMagHigh and pMagHigh pairs occurs, and *E. coli* cells will aggregate together and settle out of solution in large clusters. This settling is dependent upon concentration of $Hg^{2+}$and thus also bioluminescence intensity. Because the blue light signal of lux occurs within the solution, so close to the Magnet elements, scattering and signal loss due to using traditional blue LED lights will be reduced. More aggregation and settling out was observed using bioluminescence due to mercury detection than with light input.

Concentrating the bacteria close to the surface could serve as a pre-concentration step useful to many biosensor configurations. When the bacterial biosensors are evenly dispersed throughout the solution, often the signal that can be measured is too weak, thus the potential to pre-concentrate sensing bacteria close to the substrate would alleviate this problem. Causing adhesion and settling out of solution in these biosensors could also help to improve the reduction of signal caused by heterogeneity in cell populations.

References

1. Hsu-Kim, H.; Kucharzyk, K. H.; Zhang, T.; Deshusses, M. A. Mechanisms regulating mercury bioavailability for methylating microorganisms in the aquatic environment: a critical review. *Environ Sci Technol*. **2013,** *47,* 2441–2456.

2. Syversen, T.; Kaur, P. The toxicology of mercury and its compounds. *J. Trace Elem. Med. Biol*. **2012**, *26,* 215-226.

3. Kim, H.J.; Jeong, H.; Lee, S.J. Synthetic biology for microbial heavy metal biosensors. *Ana. and Bioana. Chem*. **2018**, *410*, 1191–1203.

4. Turdean, G.L. Design and development of biosensors for the detection of heavy metal toxicity. *Int. J. Electrochem.* **2011**, 1-15.

5. Barkay T.; Wagner-Döbler I. Microbial transformations of mercury: Potentials, challenges, and achievements in controlling mercury toxicity in the environment. In *Adv. in Appl. Microbiol.*; Allen I., Laskin J.W.B., Geoffrey M.G., Eds.; Academic Press: 2005, pp 1-52.

6. Rensing, C.; Maier, M. Issues underlying use of biosensors to measure metal bioavailability. *Ecotoxicol. Environ. Saf.* **2003**, *56*, 140-147.

7. Condee, C. W.; Summers, A.O. A mer-lux transcriptional fusion for real-time examination of in vivo gene expression kinetics and promoter response to altered superhelicity. *J Bacteriol.* **1992***, 24,* 8094–8101.

8. Brown, N.L.; Stoyanov, J.V.; Kidd, S.P.; Hobman, J.L. The MerR family of transcriptional regulators. *FEMS Microbiol Rev.* **2003**, *2-3*, 145–63.

9. Guo, H.-B.; Johs, A.; Parks, J. M.; Olliff, L.; Miller, S.M.; Summers, A. O.; Liang, L.; Smith, J. C. Structure and Conformational Dynamics of the Metalloregulator MerR upon Binding of Hg(II). *Journal of Molecular Biology.* **2010,** *4*, 555-568.

10. Luciferase-CreativeEnzymes. https://www.creative-enzymes.com/similar/luciferase_418.html (accessed Mar 30, 2019).

11. Gutierrez, J.C.; Amaro, F.; Martin-Gonzalez, A. Heavy metal whole-cell biosensors using eukaryotic microorganisms: an updated critical review. *Front. Microbiol.* **2015,** *6*.

12. Huang, C.W.; Yang, S.H.; Sun, M.W.; Liao, V.H.; Development of a set of bacterial biosensors for simultaneously detecting arsenic and mercury in groundwater. *Environ. Sci. Pollut. Res. Int.* **2015,** *22*, 10206-13.

13. Chen, F.; Wegner, S. V. Blue Light Switchable Bacterial Adhesion as a Key Step toward the Design of Biofilms. *ACS Synth. Bio*. **2017**, *6*, 2170-2174.

14. Kawano, F.; Suzuki, H.; Furuya, A.; Sato, M. Engineered pairs of distinct photoswitches for optogenetic control of cellular proteins. *Nature Comm.* **2015**, 1-8.

15. Rice, J. J.; Daugherty, P. S.; Directed evolution of a biterminal bacterial display scaffold enhances the display of diverse peptides. *Protein Engineering, Design, & Selection*. **2008**, *7,* 435-442.

16. Laganenka, L.; Colin, R.; Sourjik, V. Chemotaxis towards autoinducer 2 mediates autoaggregation in *Escherichia coli*. *Nature Comm*. **2016**, 1-10.

17. Hasman, H.; Chakraborty, T.; Klemm, P. Antigen-43-Mediated Autoaggregation of *Escherichia coli* is Blocked by Fimbriation. *J. Baterio.* **1999**, *181*, 4834-41.

18. Armbruster, D.A.; Pry, T. Limit of Blank, Limit of Detection and Limit of Quantitation. *Clin Biochem Rev.* **2008**, *29*, S49–S52.

19. Beloin, C.; Roux, A.; Ghigo, J-M. *Escherichia coli* biofilms. *Curr Top Microbiol Immunol.* **2008,** *322,* 249-289.

20. Donlan, R.M. Biofilm Formation: A Clinically Relevant Microbiological Process. *Clinical Infectious Diseases.* **2001,** *33,* 1387-92.

21. Kostylev, M.; Otwell, A.E.; Richardson, R.E.; Suzuki, Y. Cloning Should Be Simple: Escherichia coli DH5α-Mediated Assembly of Multiple DNA Fragments with Short End Homologies. *PLoS One.* **2015,** *10.*